Properties of waste gneiss powder used to design eco-friendly cement mortar

Tchedele Langollo Yannick, Matateyou Josephine Fleure, Robert Mba Eboe, Taypondou Darman Japhet, Atsafoue Donfack Sandrine, Abende Sayom Yvan Reynolds, Keyangue Tchouata Jules Hermann

JMST Advances

Properties of waste gneiss powder used to design eco-friendly cement mortar

--Manuscript Draft--

Manuscript Number:	JMAD-D-23-00012R1
Full Title:	Properties of waste gneiss powder used to design eco-friendly cement mortar
Article Type:	Letters
Funding Information:	
Abstract:	The present work concerns the determination of the geological setting of a metamorphic rock quarry in operation for the production of aggregates and the valorization of the drilling waste as a cement additive. The aim is to identify the parameters that determine the composition of the geomaterial employed, highlight that composition, and investigate its pozzolanic activity. The structural study reveals that major discontinuities are oriented N180°. The minerals identified by microscopy and mineralogical investigations are quartz (Qt), plagioclase (Pl), mica (Mi), muscovite (Mu), orthopyroxene (Px), and biotite (Bt) which are characteristic of Gneiss. After that, 10 boreholes made for blasting provided the waste gneiss powder needed. The collected samples are homogenized and then used as a partial substitute for cement from 0 to 50% with 10% intervals, for the formulation of mortars. Depending on these percentages' substitution, the setting time increases from 225 to 285 min, and the water absorption decreases from 6.05% to 2.36% at 28 days of curing. Moreover, the filler effect is underlined at 10% substitution by flexural strength enhancements of 2.22% and 1.89% between 2 and 7 days of cure. At 28 days, the compressive strengths fall from -3.33% to -20.00% for 10% and 50% substitution, respectively. The parameters that governed all of these behaviors are mainly the filler effect, the reduction in the amount of cement that increases the w/c ratio, and the size of the gneiss fines and sand used. In general, mechanical results decrease with the percentage of substitution, but the difference compared to the control specimen remains largely below the percentage substituted. The findings of this study set the groundwork for the recovery of dust from gneiss quarries as cementitious addition, as well as the limitations of this recovery.
Corresponding Author:	YANNICK TCHEDELE LANGOLLO Université de Ngaoundéré: Universite de Ngaoundere Yaoundé, Centre CAMEROON
Corresponding Author Secondary Information:	
Corresponding Author's Institution:	Université de Ngaoundéré: Universite de Ngaoundere
Corresponding Author's Secondary Institution:	
First Author:	TCHEDELE LANGOLLO YANNICK
First Author Secondary Information:	
Order of Authors:	TCHEDELE LANGOLLO YANNICK
	Matateyou Josephine Fleure

	Mba Eboe Robert
	Taypondou Darman Japhet
	Atsafoue Donfack Sandrine
	Abende Sayom Yvan Reynolds
	Keyangue Tchouata Jules Hermann
Order of Authors Secondary Information:	
Author Comments:	

Properties of waste gneiss powder used to design eco-friendly cement mortar

Tchedele Langollo Yannick [1], Matateyou Josephine Fleure [1], Robert Mba Eboe [2], Taypondou Darman Japhet [1], Atsafoue Donfack Sandrine [1], Abende Sayom Yvan Reynolds [1], Keyangue Tchouata Jules Hermann [1].

1) University of Ngaoundéré, Ngaoundéré, Cameroon.
2) University of Douala, Douala, Cameroon.

Corresponding Author: Tchedele Langollo Yannick (**Institutional e-mail:** yannick.tchedele@univ-ndere.cm)

Abstract

The present work concerns the determination of the geological setting of a metamorphic rock quarry in operation for the production of aggregates and the valorization of the drilling waste as a cement additive. The aim is to identify the parameters that determine the composition of the geomaterial employed, highlight that composition, and investigate its pozzolanic activity. The structural study reveals that major discontinuities are oriented N180°. The minerals identified by microscopy and mineralogical investigations are quartz (Qt), plagioclase (Pl), mica (Mi), muscovite (Mu), orthopyroxene (Px), and biotite (Bt) which are characteristic of Gneiss. After that, 10 boreholes made for blasting provided the waste gneiss powder needed. The collected samples are homogenized and then used as a partial substitute for cement from 0 to 50% with 10% intervals, for the formulation of mortars. Depending on these percentages' substitution, the setting time increases from 225 to 285 min, and the water absorption decreases from 6.05% to 2.36% at 28 days of curing. Moreover, the filler effect is underlined at 10% substitution by flexural strength enhancements of 2.22% and 1.89% between 2 and 7 days of cure. At 28 days, the compressive strengths fall from -3.33% to -20.00% for 10% and 50% substitution, respectively. The parameters that governed all of these behaviors are mainly the filler effect, the reduction in the amount of cement that increases the w/c ratio, and the size of the gneiss fines and sand used. In general, mechanical results decrease with the percentage of substitution, but the difference compared to the control specimen remains largely below the percentage substituted. The findings of this study set the groundwork for the recovery of dust from gneiss quarries as cementitious addition, as well as the limitations of this recovery.

Keywords: geological setting; Cement addition; strength; setting time; mineralogy.

1. Introduction

Dust is the term used to describe particles in the air with a diameter of fewer than 1000 microns. They are naturally present in the atmosphere and can be: natural or of human origin. In the aggregate industry, the term "dust" applies to solid, inert, non-water-soluble particles with a diameter between 0 and 40 microns [1]. The term "dust" is sometimes replaced by "fine" for elements with a diameter of less than 80 µm, which corresponds to the lower limit of sandy particles. For aggregate quarries, fines are non-biodegradable waste. Their emission is a source of air and soil pollution. The presence of fines in the air causes eye infections and asthma problems. Soil pollution is caused by the closing of soil pores, which limits water infiltration and therefore groundwater recharge and reduces the fertility of the soil [2].

To overcome the problem posed by the emission of fines by the industry, many studies have been carried out to valorize them in the manufacture of cement materials. In this vein, work on iron powder residues [3], glass waste fines [4, 5], basalt fines [6, 7], granite fines [2, 8, 9], and marble fines [10, 11] among others [12, 13], used as partial replacement of cement mainly, have improved the mechanical properties of mortars and concretes. The fines thus used in cement allowed the definition of the supplementary cementing materials (SCMs) class, which includes fly ash, silica fume, natural slag, blast furnace slag, and limestone powder [14]. These materials, generally industrial by-products, are therefore considered as secondary raw materials (SRM) which, according to the literature review by Martinez et al [15], had a variable effect on consistency, compressive strength, and carbonation penetration. In contrast, their use has proved to be beneficial in terms of water absorption, chloride penetration, and CO^2 emissions. Holland et al. [16] showed that the nature of these additions affects the corrosion of concrete, while the work of Habert et al., 2014 [17] was limited to the evaluation of the environmental impact of these SCMs by the analysis of the life cycles of materials. Other materials of organic origin, once calcined and ground, have also proven their worth in the manufacture of ultrahigh-performance concrete (UHPC). These are Rice Husk Ash and Palm Oil Ash [18].

The diversity of materials studied in previous work suggests that fines from a wider range of materials could have a beneficial effect on cementitious matrices. Following this order of ideas, this work will consist in valorizing the gneiss dust emitted by a quarry in Cameroon, as a cement additive in mortars and studying its properties. It will thus be a question of locating the quarry, bringing out some characteristics of the gneissic massif (macroscopic description, petrology,

mineralogy, structural), taking and characterizing the waste gneiss powder (granulometric analysis, chemistry, mineralogy), characterizing the anhydrous cement, preparing the cement paste and mortar specimens and of determining the physical-mechanical and mineralogical properties according to the standards.

This work aims to characterize a gneiss sample, show the engineering properties of gneiss powder in cement matrices, and rule on the pozzolanic effect of those to respond to the abusive valorization of this waste in Gneiss quarries by the productions of blocs and other cement derivatives under the sole pretext that they have the same physical aspect as Portland cement.

2. Location of the Gneiss quarry

The gneiss samples were taken from a quarry in operation. It is located in the Centre region, in the Mfoundi department, in the district of YAOUNDE I, in the village of NKOLOM-NDOM, and more precisely at NKOLMEKOK-NYOM II. Figure 1 shows the location of the quarry.

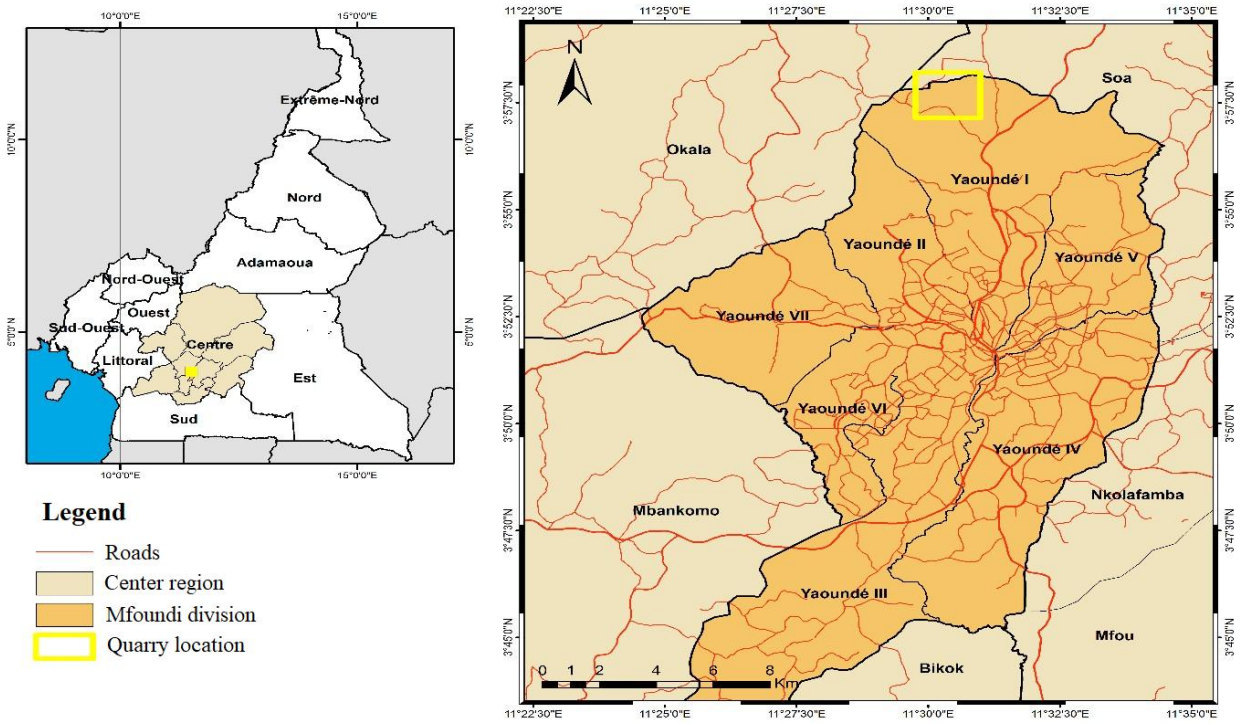

Figure 1: Quarry location

3. Geological context

The Precambrian basement of southern Cameroon comprises several metamorphic series [19]. The Yaoundé series, affected by the Pan-African orogeny (600 and 500 Ma), is mainly

formed of gneisses and garnet migmatites, derived from ancient granitized and metamorphosed sediments [20]. This series is constituted of two major migmatitic units: a metasedimentary unit or paragneiss and a metaplutonic unit or orthogneiss [21]. The paragneisses are essentially constituted of garnet and kyanite gneisses, garnet and plagioclase gneisses, marbles, and scapolite rocks. Pyriclasites intruding the metasedimentary unit, garnet pyribolites, pyroxenites, and biotiterich rocks characterize the orthogneiss [20, 22]. It is this last group that constitutes the substratum of the NKOLMEKOK-NYOM quarry. II. Figure 2 shows the geological setting of the study area.

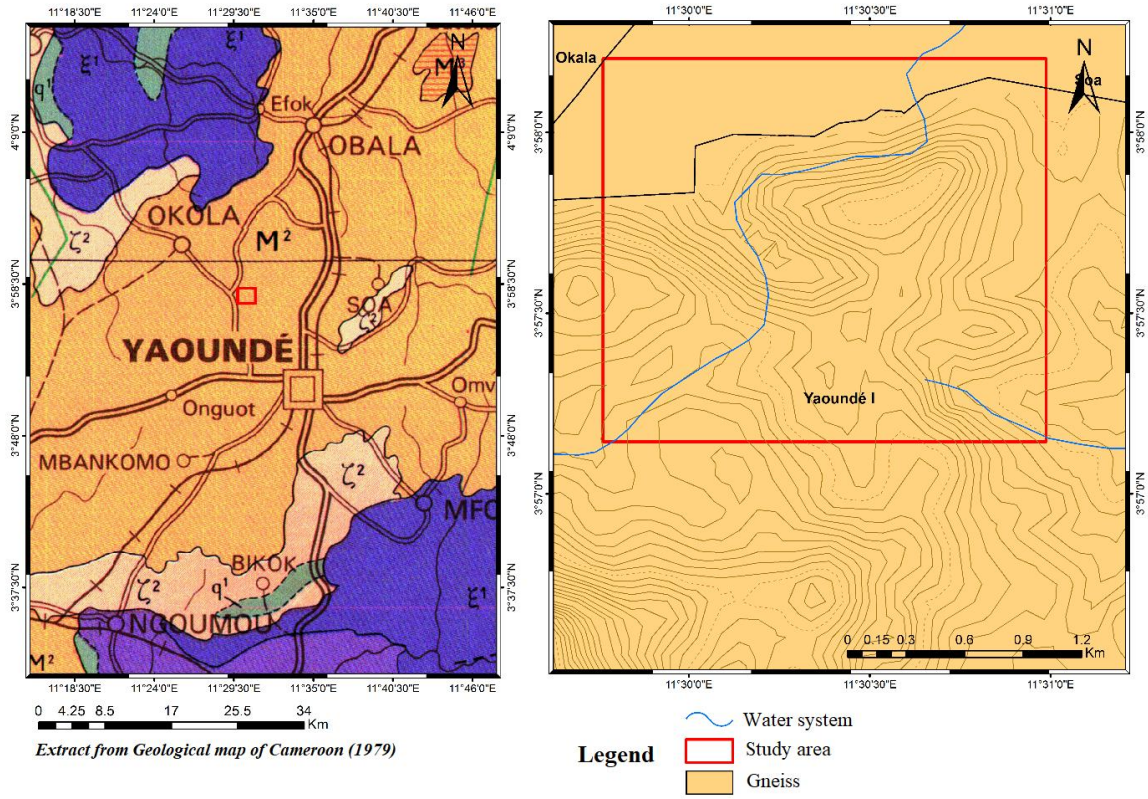

Figure 2: Geological map of the quarry

4. Materials and Methods

4.1. Materials

4.1.1. Waste Gneiss power

The gneiss powder waste was collected during the drilling operations. In this process, a large amount of dust is emitted. This dust is evacuated outside the borehole by compressed air circulation. Emissions are fairly well controlled by installing a dust collector on the drill rig. The fines are collected in bags during the drilling of the holes planned for a blasting operation and then taken to the laboratory for the work. To obtain a representative sample, the samples from each borehole are mixed in equal proportions and oven-dried at 105 °C for 24 hours.

4.1.2. Cement

The choice of cement to be used was the ROBUST 42.5R type CPJ CEM II/A-P 42.5R of the company DANGOTE in Douala because it is the most used in Cameroon. It complies with the NF EN 197-1 [23] standard presented in Table 1.

Table 1: Characteristics of the cement used [23]

Cement	physical characteristics		Chemical characteristics	mechanical characteristics	
DANGOTE 42.5R	Initial setting time (min)	Final setting time (min)	80 - 94 % of clinker 6-20% P (natural pozzolan) 0-5% secondary constituents.	Compressive strength (Mpa)	
				2 days	28 days
	> 30	< 600		≥ 20	≥ 42.5 ≤ 62.5

4.1.3. Sand

The sand used is from the banks of the Sanaga River. It was washed through the sieves of an 80-µm screen to remove the fine particles. The sand was dried in an oven for 24 h at 105 °C and sieved in different fractions with respect to the European Committee of Standardization CEN [24] for normal sand. The resulting grain size curve is presented in Figure 3.

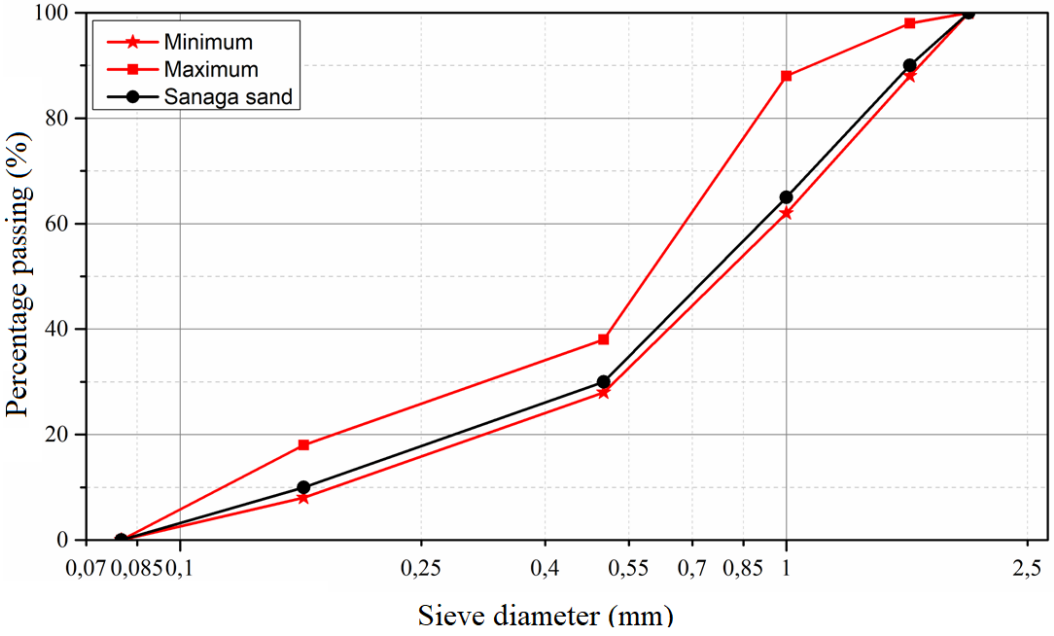

Figure 3: Granulometric curve of standardized sand according to CEN

4.2. Methods

4.2.1. Petrography

Thin sections are made on the different gneiss facies samples at the Institute for Mining and Geological Research of (Yaoundé, Cameroon). Microscopic observations are done under a polarized microscope of brand LEITZ WETZLAR observed at the laboratory of Petrology and Magmatism of the Geosciences of Deep Formations and Applications, University of Yaounde I.

4.2.2. X-Ray Fluorescence Spectrometry (XRF)

For XRF analysis, a hXRF Niton XL3t980 analyzer (equipped with an Ag-Anode 50 kV X-ray tube and Silicon-Drift-Detector 8 mm spot was used. The raw data were plotted in spectra, where x-axes represent element-specific fluorescence energy (unit keV), and y-axes quantify counts of photons (unit cps) received by the detector. Detection is possible for most of the elements with atomic numbers ranging from 12 Magnesium to 92 (Uranium). A 21 silicon-based standards so-called Certified Reference Material (CRM), filled in cups and covered with 4 µm polypropylene film were measured by hXRF device-specific mode (mining/mineral mode). The measured values were plotted using a trend line equation and the "fitting coefficient" R^2 (correlation coefficients) was determined. Afterward, a classification was made according to the quality of the regression line and the distribution of the data. XRF was performed on the waste gneiss powder.

4.2.3. X-Ray Diffractometry (XRD)

XRD measurements were performed using a D8 Brucker -AXS diffractometer equipped with Lynx eye position-sensitive detector, with Cu Kα ʎCu = 1.54056 Å radiation operated at 40 kV and 40 mA, increment 0.013° 2Θ, and a measuring time per step of 30 s. The diffraction patterns were collected in the 2 theta range from 7.5- 90°. Qualitative analysis of the phase composition of the powder samples was conducted using the PDF-2 2007 release software and X'Pert High Score Plus. XRD was performed on the raw materials (sands) at first and on the mortars at 28 curing days, to identify the hydrated products.

4.2.4. Particle size analysis by sieving

The granulometric analysis is defined by the standards [25, 26]. The following formulas were used in the context of the realization of this test:

- Percentage of cumulative sieves P (%):

$$\mathbf{P\ (\%) = 100 - r\ (\%)} \qquad \mathbf{(1)}$$

- The percentage of cumulative refusals for each sample type is denoted r (%) and is determined as follows:

$$\mathbf{r(\%) = (R/M) \times 100} \qquad \mathbf{(2)}$$

With:

R: the mass of accumulated refusals in grams.

M: the mass of the test sample for each sample

4.2.5. Cement bulk density test

The bulk density of the cement is determined following the standard [27], the bulk density of anhydrous cement is also obtained by applying the following formula:

$$\boldsymbol{\rho}_a = \frac{M1-M0}{v} \qquad (2)$$

With :

ρ: bulk density;

M1: Mass of the filled container (container + sand);

M0: Mass of the empty container;

v: Volume of the container.

4.2.6. Specific gravity of cement

The specific weight (Dr) of cement is determined following the standard [28]. It is calculated by expression (2):

$$D_r = \frac{M_2+M_1}{(M_2-M_1)-(M_3-M_4)} \qquad (2)$$

With :

M_1 = Mass of empty pycnometer (g);

M_2 = mass of pycnometer + material (g);

M_3 = Mass of pycnometer + material + paraffin (g);

M_4 = Mass of pycnometer + paraffin (g);

The specific gravity (D_S) is obtained by multiplying the actual density (Dr) by the paraffin density (γ_l).

4.2.7. Blaine Specific Surface of Cement

The fineness of cement is measured as the specific surface area using the following relationship [29]:

$$SSB = k \times \frac{\sqrt{e^3} \times \sqrt{t}}{\rho\,(1-e) \times \sqrt{0{,}1n}} \quad (3)$$

K is calculated as follows:

$$k = SSB_{Connu} \times \frac{\rho\,(1-e) \times \sqrt{0{,}1n}}{\sqrt{e^3} \times \sqrt{t}} \quad (4)$$

With :

K = constant calculated by the laboratory (K = 2.4431);

t = time in seconds, v = 1.8598;

e = porosity of the bed e=0.500;

P = density of the cement in g/cm^3;

n = viscosity of the air at the temperature of the test room;

SSB = in cm²/g.

4.2.8. Method of calculation of cement indices

The most commonly used indices in cement analysis are the Lime Saturation Factor (LSF), Silica Modulus (SM), Alumina Modulus (AM), and Hydraulic Modulus (HM) [30]. They are calculated using the following formulas:

$$\text{HM} = \frac{CaO}{SiO_2 + Al_2O_3 + Fe_2O_3} \quad (5)$$

$$\text{SM} = \frac{SiO_2}{Al_2O_3 + Fe_2O_3} \quad (6)$$

$$\text{AM} = \frac{Al_2O_3}{Fe_2O_3} \quad (7)$$

$$\text{LSF} = \frac{CaO - 0{,}7SO_3}{2{,}8SiO_2 + 1{,}2Al_2O_3 + 0{,}65Fe_2O_3} \quad (8)$$

4.2.9. Bogue calculation methods

The Bogue calculation method [31], is used to estimate the contents of the four main minerals in the clinker. The corresponding formula (in mass %) are:

$$C_3S = 4{,}071CaO - 7{,}602SiO_2 - 6{,}718Al_2O_3 - 1{,}430Fe_2O_3 - 2{,}852SO_3 \quad (9)$$

$$C_2S = 2{,}867SiO_2 - 0{,}7544C_3S \quad (10)$$

$$C_3A = 2.65Al_2O_3 - 1.692Fe_2O_3 \quad (11)$$

$$C_4AF = 3{,}043Fe_2O_3 \quad (12)$$

4.2.10. Production of mortar specimens

The mortar specimens were made according to EN 196-1 [24] with dimensions of 4x4x16 cm^3. From the formulation of the normal mortar, at w/c=0.5, the sand used was basalt sand (SB01), granite sand (SGR02), gneiss sand (SGN03), Canada sand (SS04), and wouri sand (SW05). The different formulations were MB01, MGR02, MGN03, MS04, and MW05 respectively for each sand used. Three specimens of each formulation were used for both the flexural strength test and the compressive strength test. A total of 54 specimens were produced, with 9 specimens of each substitution %, three of which will be used for tests at 2, 7, and 28 days. The quantities used are found in Table 2.

Table 2: Materials used for the preparation of the gneiss dust mortar specimens

Percentage of waste gneiss powder (%)	Cement (g)	Mass of waste gneiss powder (g)	Standardized sand (g)	Water mass (g)
0	500	0	1350	225
10	450	50	1350	225
20	400	100	1350	225
30	350	150	1350	225
40	300	200	1350	225
50	250	250	1350	225

4.2.11. Setting time

The setting time test is performed with the Vicat apparatus on the cement paste at normal consistency. The initial setting time, the final setting time, and then the setting are carried out following Standard [32].

4.2.12. Water absorption

The water absorption (a_b) of each 4x4x16 cm^3 mortar specimen made at 2, 7, and 28 days is expressed by Equation 3 according to the standard ASTM C642 – 13 [33]:

$$a_b = \frac{m_h - m_s}{m_s} \times 100 \qquad (3)$$

with

$\mathbf{a_b}$ = water absorption

$\mathbf{m_s}$ = dry mass

$\mathbf{m_h}$ = wet mass

4.2.12. Mechanical tests

The flexural strength test (3-point test) was carried out on three 4x4x16 cm^3 prismatic mortar specimens, for each formulation, at 2, 7, and 28 days of cure. In the end, the strength allowed is the average of the three values obtained. This test is performed according to EN 196-1 [24], using an ELE ADR-Auto hydraulic press and applying the formula (4):

$$\boldsymbol{R_t = \frac{1{,}5 \times P \times L}{b^3}} \quad \textbf{(4)}$$

Where
R_t = Flexural Strength MPa
L = distance between the lower support in mm
P = breaking load in N
b = thickness of the specimen (b = 40 mm)

The test set-up is shown in Figure 4.

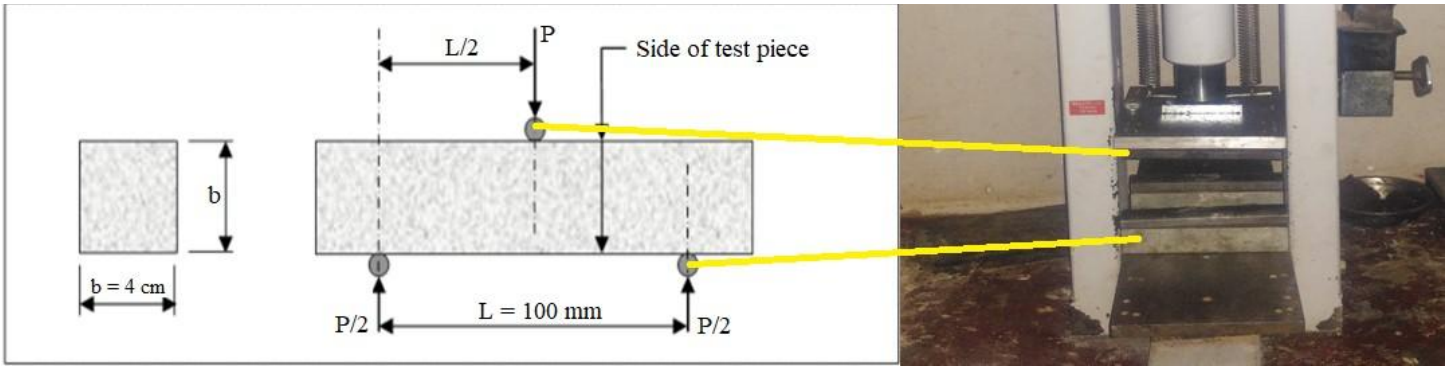

Figure 4: Device for flexural tensile strength testing

The compressive strength test is carried out on each half of the specimen used for the flexural test on the same dates. It is carried out with the same instrument, but this time it is equipped for compression testing (Figure 5). The compressive strength is calculated using the formula 6:

$$\boldsymbol{R_c = \frac{P}{S}} \quad \textbf{(5)}$$

With
R_c = compressive strength MPa
P = breaking load N
S = specimen section in mm^2 (S = 1600 mm^2)

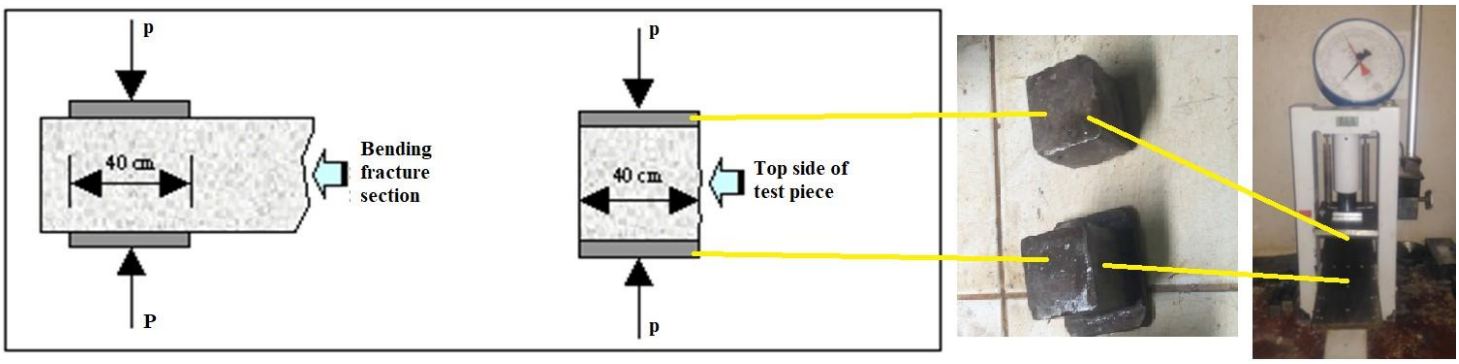

Figure 5: Compressive strength testing device

5. Results and discussion

5.1. Geological setting of the quarry and sampling

5.1.1. Macroscopic description of the rocks of the Nkolmekok-Nyom II quarry.

The target quarry massif is a crystalline metamorphic rock. It is formed of minerals of millimeter to centimeter sizes arranged in beds. One can clearly distinguish an alternation of quasiparallel bands of dark color, rich in ferromagnesian minerals (micas, amphiboles, or others), and clear bands (white or pinkish) of quartz and feldspars which are the result of generalized metamorphism The rock matrix observed in Figure 6 consists of three parts: the quartz veins, an unfused part, and a fused part that includes the minerals. These parallel superimposed sets are intersected by a fault.

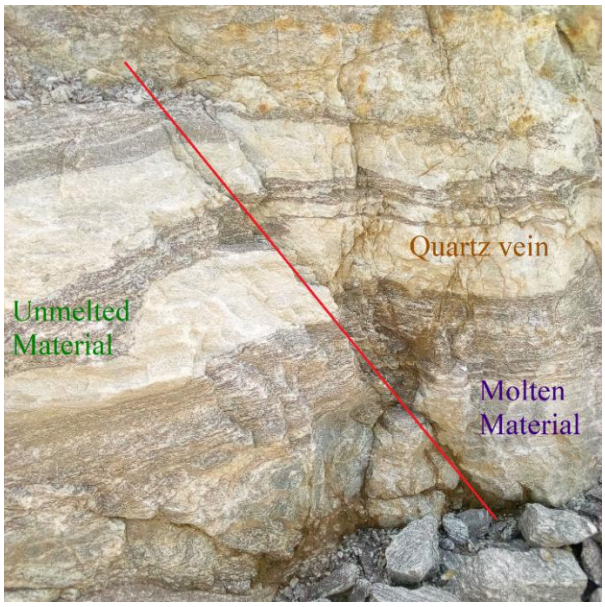

Figure 6: Profile of the lithological facies observed in the outcrop

The work of Mambou et al [34] also identified on the metamorphic rocks of the region, fruste foliation, and an alternation of light and dark rocks, indicating that it is Gneiss. The presence of feldspar has been discovered by those researchers, as well as quartz veins formed as a result of quartz-feldspathic intrusion plugged cracks created during the metamorphism of endogenous rocks. These observations are characteristic of the gneiss observed in the Pan-African metasedimentary formations at the northern margin of the Congo Craton [35].

5.1.2. Structural configuration of the rocky massif

The different observations made on the massif (Figure 7) highlight structures such as:

- The veins: are mainly represented by quartz veins.
- Folds: These are undulations resulting from the bending or twisting of the rock.
- The foliation: it is the noticed alternation of light and dark beds on the massif.
- The joints: represent the ruptures without displacement appreciated by the naked eye on the side of the rock.
- Breaks: these are the fractures of the ground with observed displacement.

Figure 7: the different deformations of the quarry

The Steering rosette shown in Figure 8 allows us to observe the orientations of major and minor discontinuities in the Nkolmekok-Nyom II quarry.

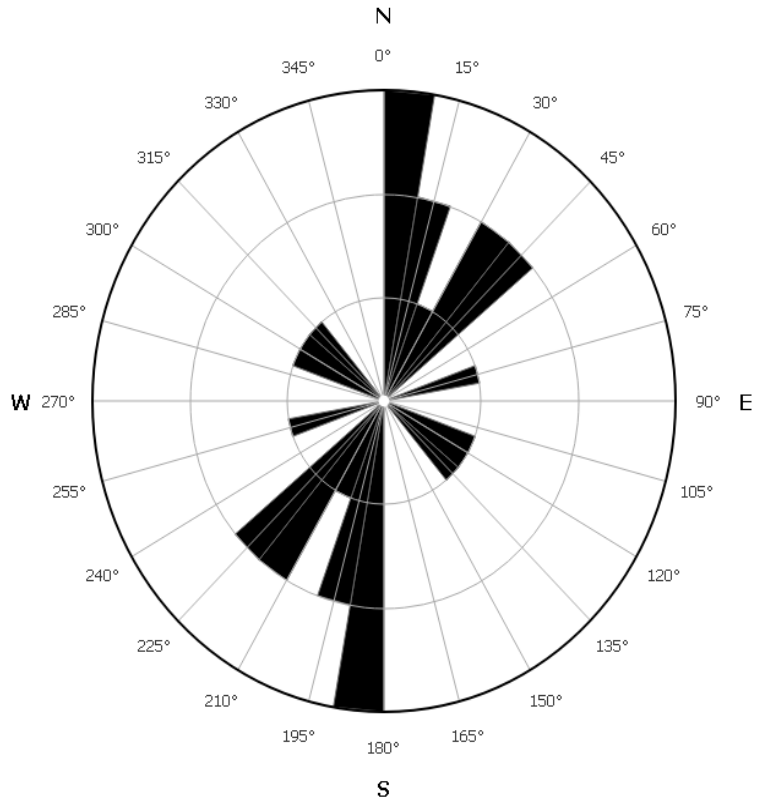

Figure 8: Steering rosette of the Nkolmekok-Nyom II quarry.

According to structural data collected in the field and plotted in Figure 8, the major orientation of these structures is N180°. The identified features are generated by tectonic movements similar to those of the Cameroon line, as they have the same direction. The same result concerning structural orientations has been obtained by Mboudou et al. [36] for Penja–Manjo pegmatites in the Pan-African orogenic belt of Cameroon. The secondary orientation of these structures is N30°-N45°. These orientations correspond to the principal structural orientation (N35°) of Cameroon [37]. A minor or tertiary orientation of the structures may also be observed, corresponding to N75° and N120°. These orientations are very rarely found in the study area.

5.1.3. Microscopic description

Three facies in the massif that are macroscopically distinct were the focus of this study. From the observations made on sample SAM1 (Figure 9), it appears that the minerals present have a mesocratic coloration, a granoblastic texture, and a mineralogical assemblage mainly composed of quartz (Qt), plagioclase (Pl), mica (Mi), muscovite (Mu), orthopyroxene (Px) and biotite (Bt). We note a strong presence of more or less oriented micas, these observations confirm the gneissic

nature of the rocks resulting from the metamorphic formation highlighted during the field investigations and presented by the literature [19-22]. This formation is identified on the northeast side of the Nkolmekok-Nyom II quarry.

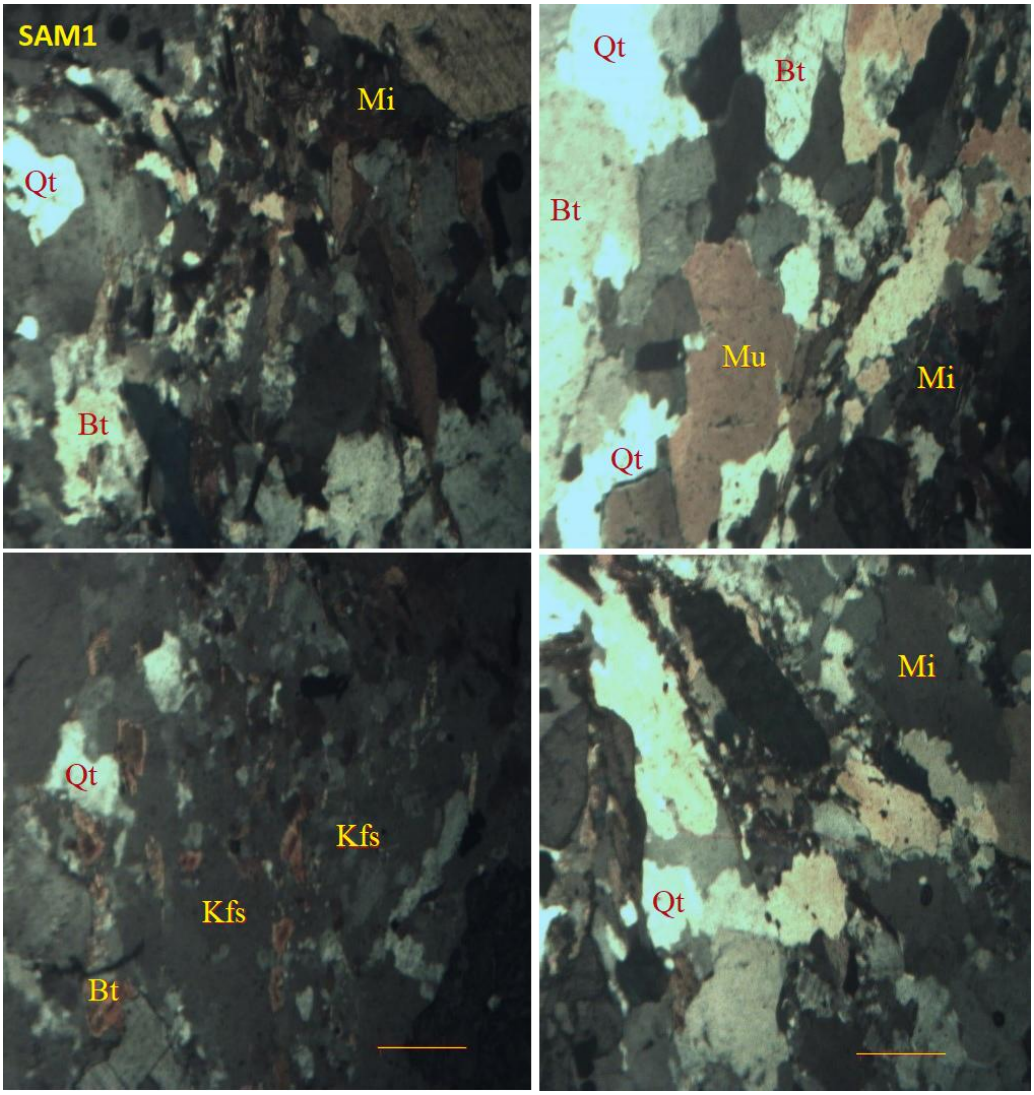

Figure 9: SAM1 thin section in LPNA

The samples SAM2 (Figure 10) and SAM3 (Figure 11) appear microscopically identical since we observed in detail that:

- Quartz (35 and 30%) is in the form of xenomorphic crystals. Some minerals are included in the garnet as well as others associated with biotite, with a size of 0.01163614mm;
- The potassium feldspar (30 and 25%) is in xenomorphic form and is associated with quartz which is mainly orthoclase, with a size of 0.03095949 mm;

- The garnet (25 and 20%) is in xenomorphic form, there is an intrusion of quartz in the garnet, strong relief (well delimited) strong relief, structure epiblastic (minerals elongated), granolipidoblastic texture. With a size of 0.06608501 mm;
- Plagioclase is in orthomorphic form a strong relief, with a size of 0.06368202 mm;
- The biotite is presented in lamellae or automorphic, lengthened parallel to the foliation. It passes from brown to light brown. The size is 0,007413204 mm;
- Opaque minerals are represented by oxides, the mineralogical assemblage of amphibolites such as Biotite (Bt) + Pyroxene (Px) + Quartz (Qt).

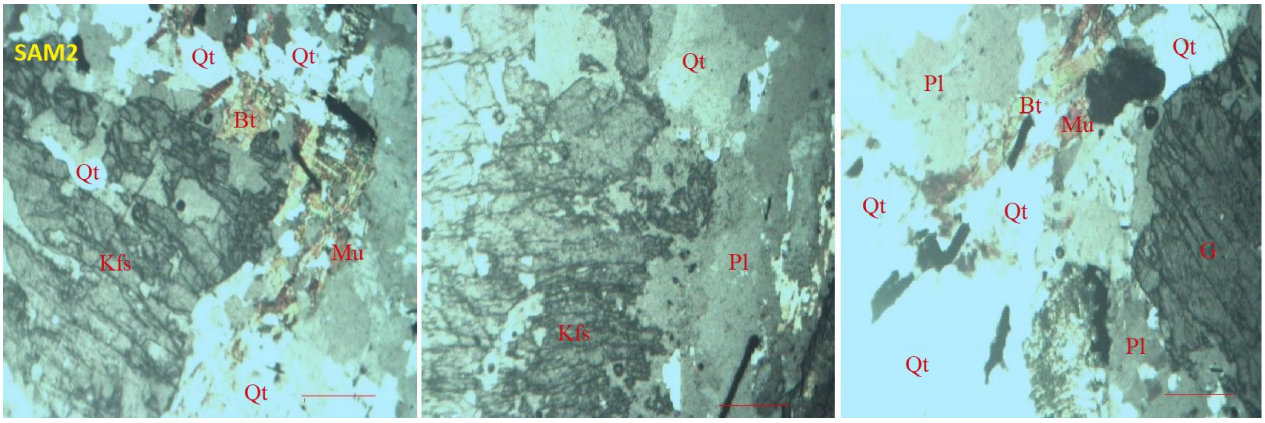

Figure 10: SAM2 thin section in LPA

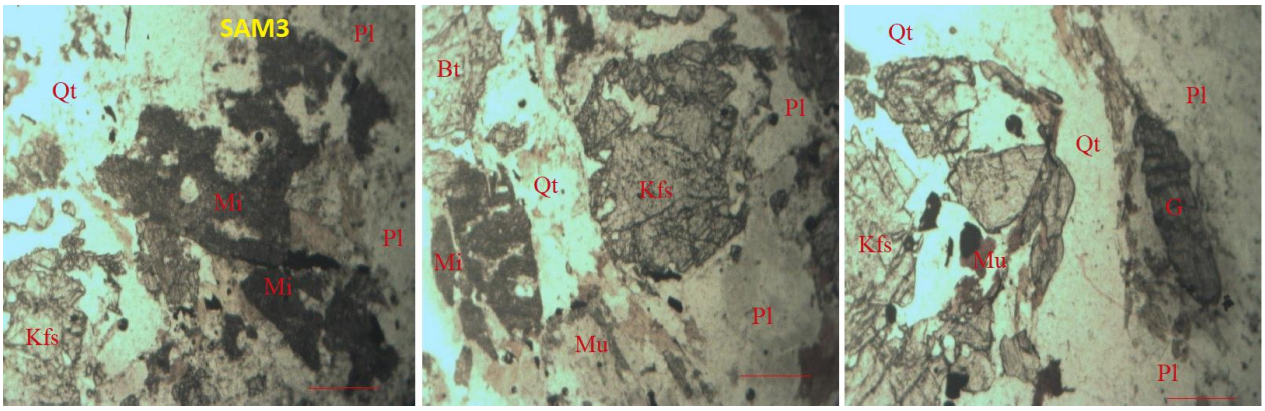

Figure 11: SAM3 thin section in LPA

In general, most of the gneissic massif in the Nkolmekock-Nyom II area outcrops in slab form. These outcrops are foliated and folded. The dark bands consist of biotite, amphibole, and ferromagnesian minerals and the light bands consist of quartz, feldspar, kyanite, and garnet. A similar finding was reached by Mambou et al. [34]. Matomb gneisses in southern Cameroon also contain quartz, biotite, muscovite, garnet, and feldspars. However, the presence of accessory minerals such as kyanite, rutile, apatite, and enstatite is also observed [38]. Fuanya et al. [39]

discovered amphibole + garnet + plagioclase feldspar + Fe oxides + quartz + biotite in south-west Cameroon; metadolerites occurred as small blocks and were characterized by a mineralogical composition dominated by plagioclase, pyroxene, and amphibole. Magnetite, hematite, quartz, biotite, and microcline were also present. As a result, it appears that the mineralogical composition of the gneiss may vary depending on latitude, determining the chemical composition likely to influence the gneiss's behavior in cementitious matrices.

5.2. Sampling

Following the sample collection process described above, the various sample collection points are shown in Figure 12 and were selected from the drill holes drilled for one blast to obtain a representative sample of the portion of the liability fired.

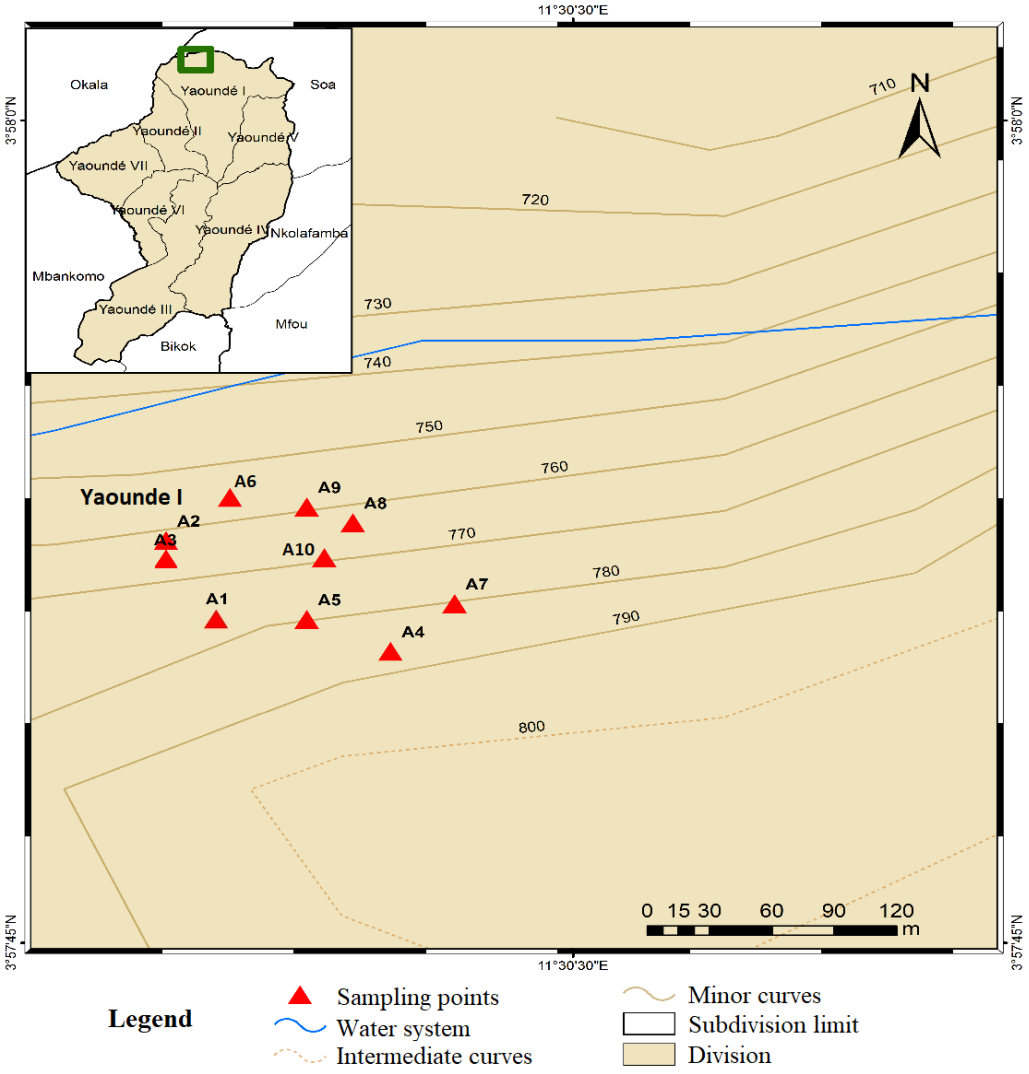

Figure 12: Sampling map

5.3. Results of chemical analysis of Gneiss facies by X-ray fluorescence

Table 3 presents the results of XRF performed on the previously identified Gneiss facies.

Table 3: XRF results on Gneiss facies

	PAF	SiO_2	Al_2O_3	Fe_2O_3	CaO	MgO	K_2O	Na_2O	SO_3	P2 O5
SAM1	0.81	56.21	13.89	8.18	1.9	2.33	3.55	1.66	0.06	0.1
SAM2	0.083	57.78	14.25	8.95	2.24	3.28	2.1	1.86	0.05	0.12
SAM3	0.79	55.47	12.56	9.02	2.21	2.55	2.12	1.8	0.05	0.1

These results show that SiO_2 is the most abundant oxide with values close and between 55.47 and 57.78%. These values are in agreement with the analysis of the thin slides which shows that quartz is the most abundant mineral (30-35%). In the second position, we find the Al_2O_3 whose value is between 12.56 and 14.25. These values are due to the contribution of Feldspar, biotite, and garnet among others. In the third position, we have the Fe_2O_3 whose value varies between 8.18 and 9.02. These values are representative of the ferromagnesian minerals present in the materials. The other base oxides are present in relatively small amounts ($\leq$3.55%) and are characteristic of minor minerals in the materials. It should be noted that, in general, the chemical composition varies very little, showing that the chemical and by extension mineralogical composition of the studied gneissic massif seems more or less uniform. These results are similar to those of Nzenti et al. [40] who carried out a thorough investigation of the gneissic formations of Yaoundé.

5.4. XRD results on Gneiss facies

XRD performed on the facies used for petrographic analysis produced the results recorded in Figure 13.

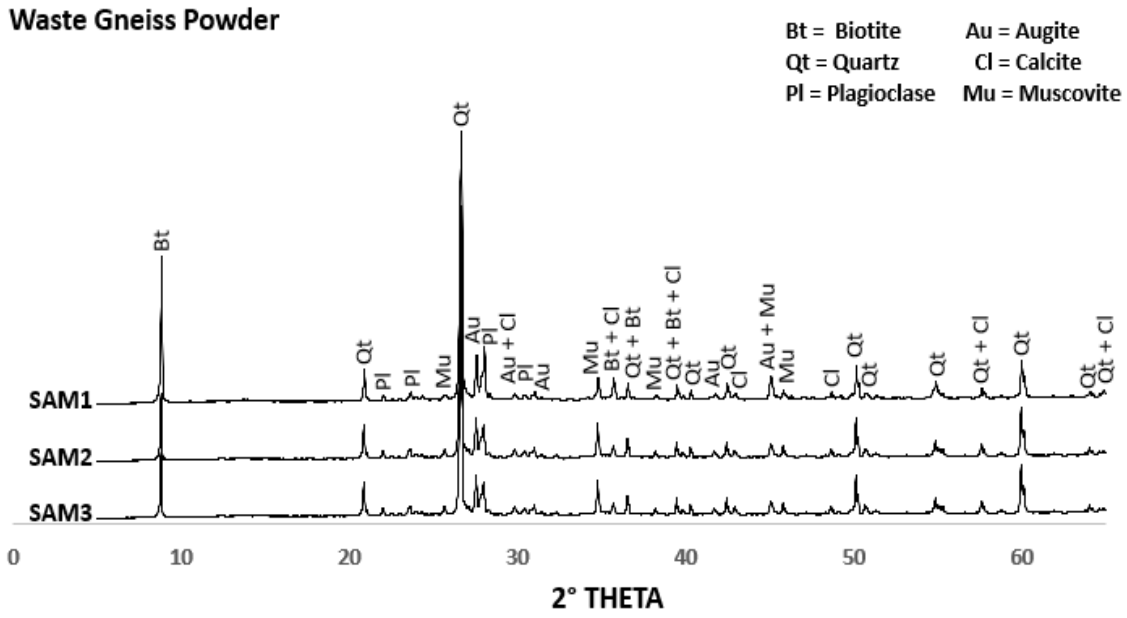

Figure 13: XRD of gneiss powders from different facies used for petrography

It is found that the different facies contain Biotite, Calcite, Quartz, Augite, Anorthite, Albite, and Muscovite. These minerals correspond to those of gneissic materials identified by numerous works [21, 22, 40] and confirm or complement the minerals identified by petrographic analysis with muscovite, calcite (light minerals), and augite (dark mineral) which is pyroxene. The presence of these minerals explains the contents of CaO (calcite), MgO (augite), and K_2 O (muscovite), obtained by XRF.

5.5. Granulometric analysis of waste gneiss powder

The particle size analysis carried out on the waste gneiss powder allowed us to draw the graph in Figure 14.

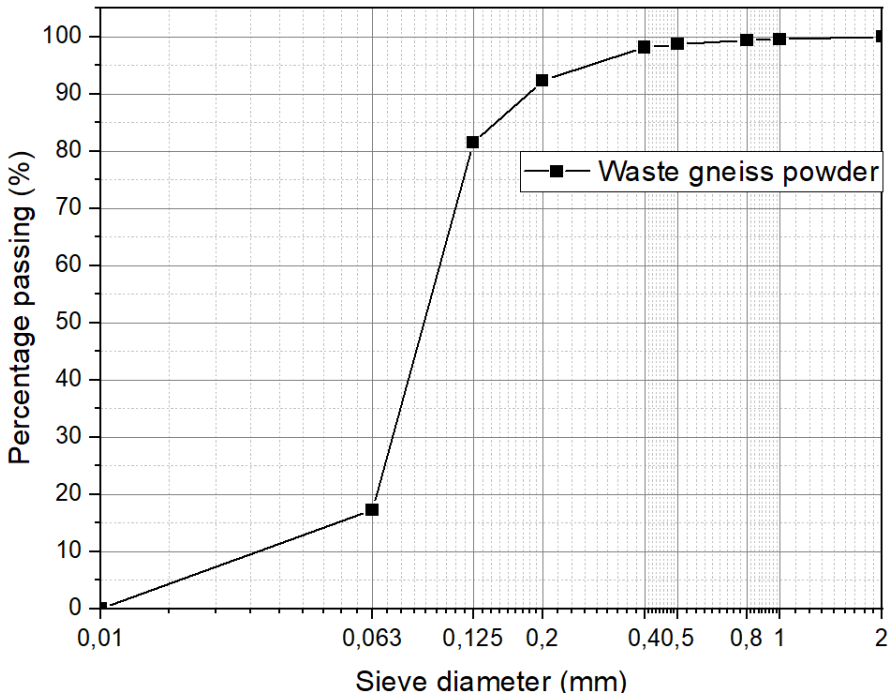

Figure 14: Granulometric analysis of waste gneiss powder

These results show that the fines content (≤ 80µm) is higher than 40%. 80% of the waste gneiss powder has a granulometry lower than 125 µm and the remaining 20% is mostly lower than 500 µm. They confirm the fact that the waste gneiss powder produced by the drilling process is largely fines that take the name of "fillers" according to the standard NF EN 12620 [41] on aggregates for concrete. Various studies have used fillers as supplementary cementing materials with a variable particle size distribution. Some [7] have used basalt powders with a particle size between 125 µm and 8mm in mortars and their results showed a decrease in compressive strength. Others [6], with a grain size between 0 and 200 µm obtained slightly decreasing compressive strengths, but increasing flexural strengths according to the additions made. The work on mortars containing waste granite powders with a grain size between 0.1 and 400 mm obtained flexural and compressive strengths that increased in some formulations. This shows that particle size plays an important mechanical role in the use of fines in cementitious matrices.

5.6. Physico-chemical properties of cement

The cement used in this section is CPJ CEM II/A-P 42.5R manufactured by the company Dangote SA. It is a composite Portland cement, with high initial strength and minimum strength at 28 days on a standardized specimen of 45 MPa. It consists of a mixture of clinker whose content is between 80-94% (CEM II/A) and secondary constituents (Pozzolan (P) + gypsum) whose content

varies from 6 to 20% [23]. The results of the physicochemical characterization are recorded in Table 4.

Table 4: Physico-chemical characteristics of cement

Cement	SiO_2	Al_2O_3	Fe_2O_3	CaO	MgO	SO_3	K_2O	Na_2O	P_2O_5	LOI	Rejection at 0.08mm (%)	Bulk density (g/cm^3)	Specific weight (g/cm^3)	SSB (cm^2/g)
OPC	18.68	5	3.31	62.88	1.04	3.78	0.36	0.35	0.11	5.94	0.59	0.91	2.98	3353

It follows that the SSB of the cement used is 3353 cm2/g, which induces a good reactivity of the latter. Duna et al. [42], obtained different results (1.26 g/m2) on the same cement, which could be explained by the fact that the work was carried out at different times. The C.P.J NC CEM II/B-P 42.5R cement used in the work of Mambou et al. [43] has a higher SSB (3425cm2/g) as well, with the same effects on reactivity. The specific gravity of the CPJ CEM II/A-P 42.5R cement, meanwhile, is 2.98 g/cm3, which is lower than those of literature [43, 44], i.e. 3.12 and 3.16 g/cm3, respectively. The rejection of the cement 0.08 mm sieve meets the standard [29] and is substantially lower than that of the dust. These results confirm that the properties of cement of the same class vary significantly from one manufacturer to another and also from one production to another.

Regarding the chemical results (XRF), CaO is the most abundant oxide (62.88%), followed by SiO_2 (18.68%), Fe_2O_3 (3.31%), Al_2O_3 (5%) and SO_3 (3.78%). The other oxides combined are in smaller amounts (sum ≤ 1.86%). The content of equivalent alkalis (Na_2O equivalent) is 0.59%. Such results are common to Portland cement and depend on the formulation of the raw meal [41, 45-47]. The SO_3 content (3.78%) follows the standard [23] which recommends a value less than or equal to 4%. Calculation of cement characteristic modulus [42] and application of Bogues formulas [31] for LSF > 0.64 produced the results in Table 5.

Tableau 5: Results of the calculation of the cement modulus and the main mineral phase content

	Cement Modulus						Mineral phase content by Bogue's formula			
Cement	LSF	HM	SM	AM	HI	LSI	C3S	C2S	C3A	C4AF
OPC	1.02	2.33	2.25	1.51	0.37	1.05	62.02	6.77	7.65	10.07

Thus, in the studied cement, the lime saturation factor (LSF) is 1.02. It reflects a good concentration of lime contributed by the main constituents (C3S, C2S, C3A, and C4AF) of these cement [47]. The current value of SM obtained (2.25), accompanied by a high LSF as in the case in point, revisits a high content of C3S (62.02%) and the distribution of lime in the other main

constituents [42]. The CPJ CEM II/A-P 42.5R cement used also has significant C3A + C4AF contents (17.72% and 13.92%). The dominant value of C3S makes this cement an Alite cement. The aluminous modulus (AM) is 1.51 and implies a heat of hydration in the average of commercial cement [42]. The value of the hydraulic modulus (HM) (2.33) refers to initial strengths that could be relatively low, as they deviate slightly from the expected range (1.7 to 2.3) and may cause swelling. The value (0.37) of the hydraulic index is also outside the range (0.4 to 0.5) recognized for good water resistance [48].

5.7. Cement paste setting time test results

The setting time test was carried out with the Vicat apparatus following standard [32]. The results are shown in Figure 15.

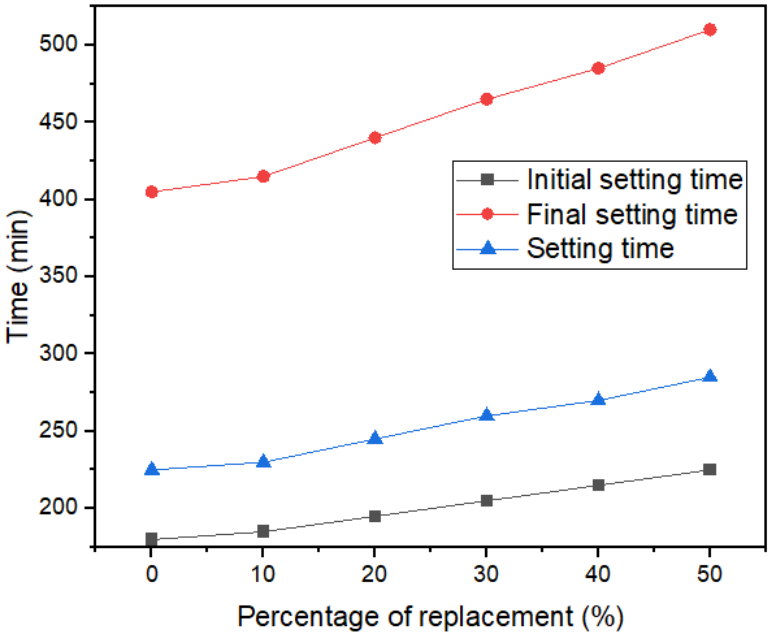

Figure 15: Setting time of the cement paste for different percentages addition of waste gneiss powder

The setting time varies from 225 min for 10% substitution to 285 min for 50% substitution. It is noted that in general, the setting time increases by 15 minutes for 10% waste gneiss powder addition. When the supplementary cementing materials do not contain minerals that influence the setting time, such as reactive sulfates, many studies [49-51] agree on the fact that the setting time is greatly influenced by the particle size of the supplementary cementing materials. Indeed, the Incorporation of recycled fine materials into the cement matrix increases the initial setting time from 20% to 63% depending upon the size fraction of recycled fine aggregate, whereas the final

setting time of the mix varies from low to high depending on the presence of organic matter, clay, etc. [49, 50].

In general, high alkali content results in a rapid setting time [52]. The increase of the setting time of cement with the addition of waste gneiss powder implies therefore the low reactivity of alkaline elements in these materials. The dispersion of cement particles in the cement paste due to the addition of waste gneiss powder may also be the cause of the setting time increase [53]. Similarly, the reduction in the quantity of cement implies an increase in the water/cement ratio (*W/C*) would also be at the origin of this increase in setting time, because according to Tchedele et al [4], the higher this ratio, the longer the setting time. All of these elements contribute to explaining the growth of the setting time observed.

5.8. Result of water absorption test on mortar specimens

The water absorption test carried out on the mortar specimens with the different percentages of addition at 2 days, 7 days, and 28 days of cure, produced the results recorded in Figure 16.

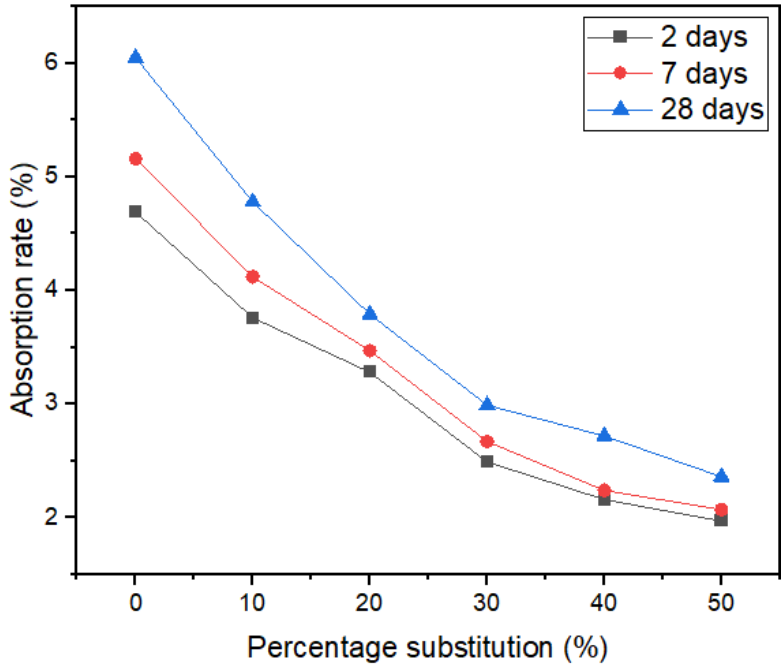

Figure 16: Water absorption of mortar specimens at different curing times

Generally speaking, water absorption increases with the duration of the cure. It contrary decreases with the increase of the waste gneiss powder content, between 2 and 28 days. Indeed, it drops from 4.69% (OPC) to 1.97% (50% addition) at 2 days, 5.16% (OPC) to 2.07% (50% addition) at 7 days, and 6.05% (OPC) to 2.36% (50% addition) at 28 curing days. This decrease corresponds to the filling of the voids by the fines of the addition (fillers). According to Li et al

[54] and Gupta et al [2], absorption is related to water-accessible porosity. This shows that the most porous composites have the highest absorption coefficients. In this sense, many works have shown microscopically that the addition of inert fines or fines that partially react with the cementitious phases has the effect of reducing the porosity of the matrix [4]. Mercury Intrusion Porosimetry (MIP) analysis in the work of Cui et al [3], also confirms the decrease in porosity with the addition of Waste Iron Tailing Powders. In contrast, the work of Ramadji et al [9] shows that the addition of granite powder increases the porosity of the mortars. This discrepancy in the results can be explained by the nature of the aggregates used. Sand with a high percentage of fines would tend to offer less space to fillers, while sand washed with an 80 µm sieve, as in this study, favors the filler effect.

5.9. Mechanical Test

5.9.1. Flexural strength results

Among the mechanical tests performed on the mortar specimens, the results of the tensile strength tests by flexion performed at 2 days, 7 days, and 28 days following EN 196-1 [24], are recorded in Figure 17.

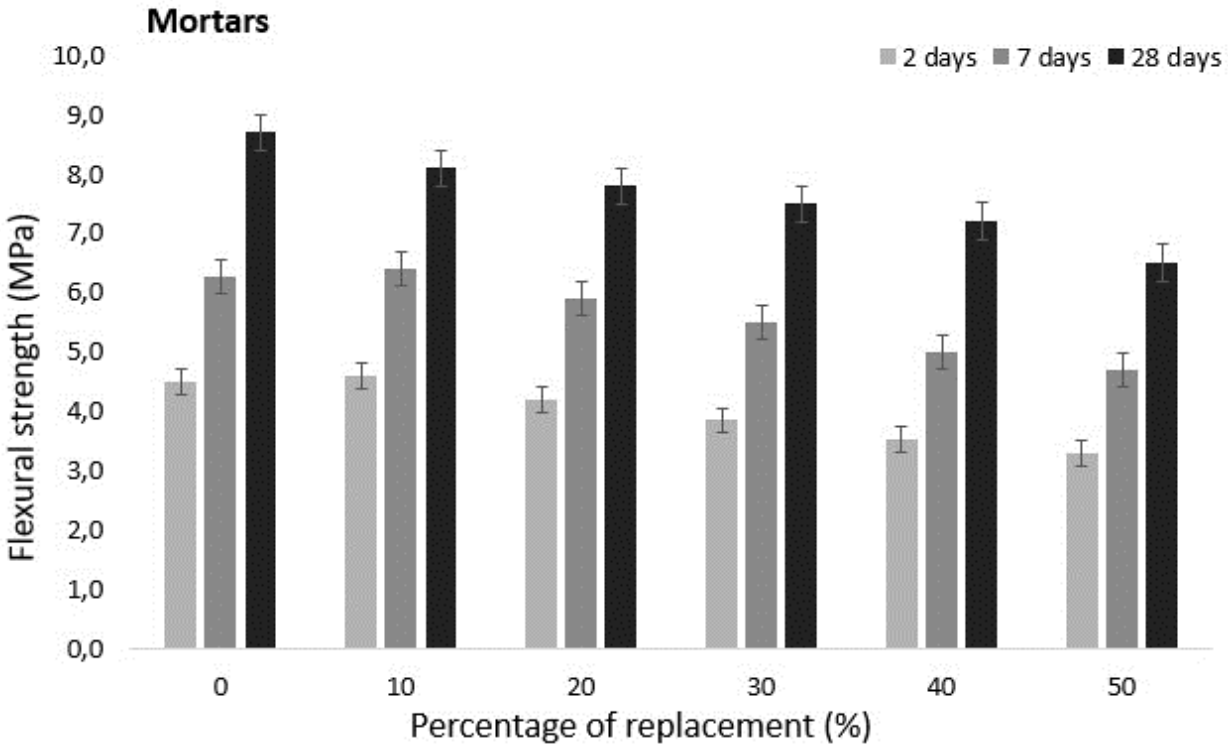

Figure 15: Flexural strength test results

These results show a monotonic decrease in strength at 28 days, while at 2 and 7 days of curing, the specimens made with 10% cement substitution show a slight increase in flexural strength compared to the control specimen. The observed trend is explained by the fact that at 28 days when the mechanical effect of the cementitious reactions is at its maximum, the reduction of cement gradually reduces the strength. This state of affairs seems to confirm the fact that the gneiss powders are inert in the cement and act mainly by the filler effect. Indeed, in addition to the observed decrease in strength, the improving effect brought by the waste gneiss powder with 10% substitution between 2 and 7 days is attributable to this filler effect [55]. The numerical variation of the flexural strength of the specimens with the addition of waste gneiss powder compared to the control specimen is shown in Table 6.

Table 6: Variation of flexural strength of mortars with waste gneiss powder added at 2, 7, and 28 days

Waste gneiss powder content (%)	Variation of flexural strength of mortars with the addition of waste gneiss powder (Mpa)		
	2 days	7 days	28 days
0	0.00	0.00	0.00
10	2.22	1.89	-6.90
20	-6.67	-6.07	-10.34
30	-14.44	-12.44	-13.79
40	-21.53	-20.40	-17.24
50	-26.67	-25.17	-25.29

It can be seen that in general, the decrease in bending strength is much smaller than the reduction of cement content in mortars and some cases even greater than the reference. The effect can be also related to the large irregularity and roughness of the surface of waste gneiss powder which can mechanical wedging in the cement matrix [6]. Moreover, works have shown that the increase in specific surface area causes the improvement of the mechanical properties of cementitious composites [56, 57]. Thus, the hydration process can be sequenced as follows: between 2 days and 7 days, the amount of C-S-H phase increases tightly filling the space between irregular grains. This allows to transfer of stress effectively through the gneiss-cement paste interface and exploits the proper strength of the gneiss. At this stage, even a slight growth to 10% substitution is observed. Then, after a relatively long hydration period (28 days), the reduction of

the quantity of cement will have the effect of reducing the mechanical strength. Here, the filler effect will no longer be sufficient to fill the strength gap caused by the reduction in cement.

5.9.2. Compressive strength results

The mechanical tests also include the compressive strength test carried out following the standard EN 196-1 [24]. The results are shown in Figure 18.

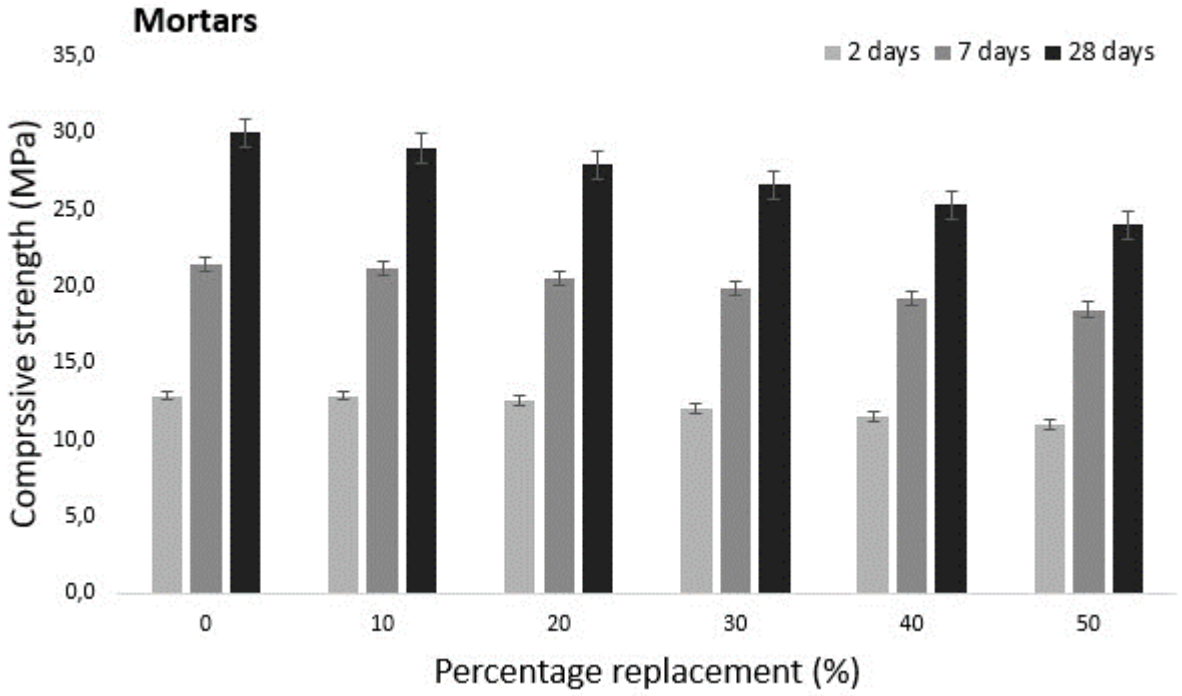

Figure 18: Compressive strength test results

From these results, it appears that the variation of 2, 7, and 28-day compressive strength of cement mortars concerning the replacement of waste gneiss powder causes the constant decrease of the compressive strength of mortar in all curing times. The most visible decrease is observed in the case of mortar with 50% replacement of cement by basalt powder, i.e. 20% at the age of 28 days, as shown in Table 7.

Table 7: Variation of compressive strength of mortars with the addition of waste gneiss powder at 2, 7, and 28 days

Waste gneiss powder content (%)	Variation of flexural strength of mortars with the addition of waste gneiss powder (Mpa)		
	2 days	7 days	28 days
0	0.00	0.00	0.00
10	0.00	-0.93	-3.33
20	-2.33	-4.21	-7.00
30	-6.98	-7.01	-11.33

40	-10.85	-10.28	-15.67
50	-14.73	-13.55	-20.00

Waste gneiss powder only acts like inert mineral admixtures reducing the strength. The main reason for decreasing strength is cement dilution [6]. Cement content decreases with the increasing amount of waste gneiss powder. It also leads to a gradual increase in the water/cement ratio. For some researchers, when the w/c increases for a constant content of cement, more water is available between the particles with more pores in hardened mortar. Increased porosity would lead to a decrease in compressive strength [58]. Other authors [3, 7, 9] agree that the decrease in strength of mortars with high doses of chemical and mineralogical admixtures was significantly affected by the segregation of the mortars, which led to their non-homogeneous structure and consequently to a reduction in strength. However, as we can observe in Table 5, this reduction is lesser than the percentage substitution of cement by waste gneiss powder as demonstrated above. These types of formulations despite some observed losses in strength can have many applications, particularly in habitat construction in less aggressive environments or for soil stabilization [59], or even in the simple but noble purpose of producing an eco-friendly cement mortar.

5.10. XRD results of mortar specimens

The XRD performed after 28 days of curing, on the mortar specimens used for the mechanical tests allowed to draw the graph in Figure 19.

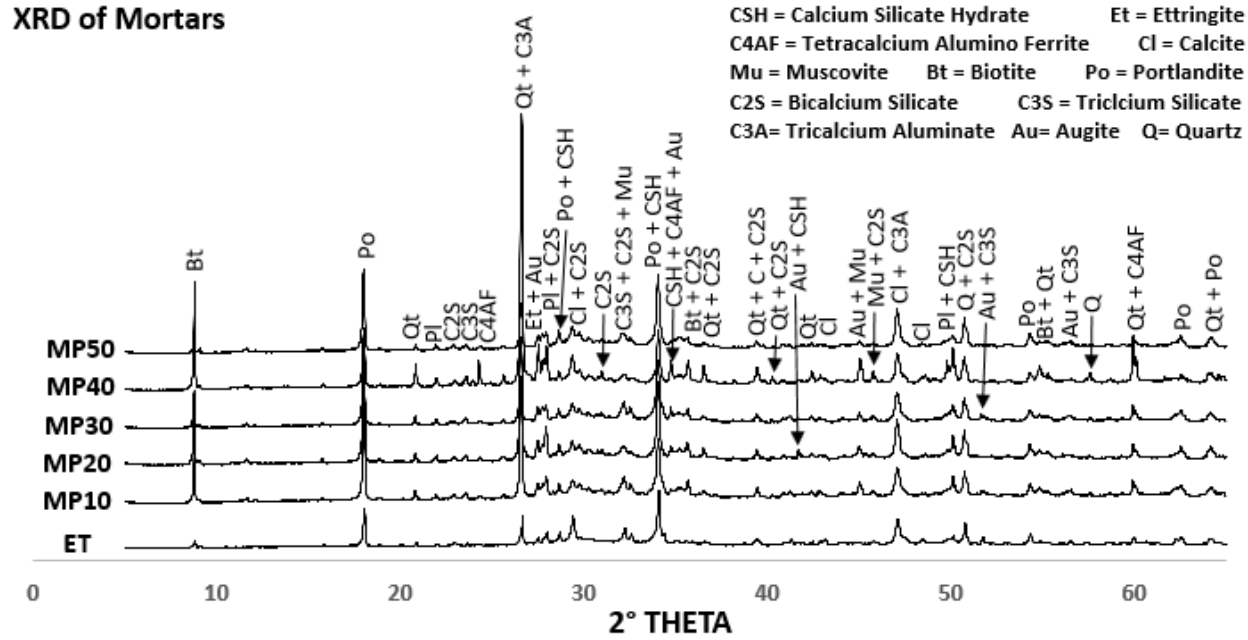

Figure 19: XRD of Mortar specimens used for mechanical tests

These results show the presence of Biotite, Albite, Portlandite, Quartz, Anorthite, Calcite, Augite, C3S, C4AF, Ettringite, C3A, CSH, and Muscovite, which are essentially the hydrated and anhydrous minerals in the cement [4] and the minerals identified by XRD performed on the waste gneiss powder (Figure 11). At first sight, these results reinforce the idea stated by some researchers [3, 7, 9], concerning the chemical inertia of some mineral additions used as a partial replacement for cement. However, the analysis of the depth of the peaks reveals that from ET (0% substitution) to MP50 (50% substitution), the Portlandite peaks increase, which suggests that the CaO provided by the waste gneiss powder becomes hydrated. C3A and C4AF peaks appear or grow with the addition. This phenomenon would also be attributable to the aluminous minerals present in the substitute material. The same is true for the dicalcium silicate peaks that grow in places. The crushed quartz would be at the origin of this growth.

It seems that, despite the previous tests that suggested inertia of the waste gneiss powder in the mortars, the mineralogical analysis reveals that they could be at the origin of some hydrates of the cement, even of some non-hydrated phases. However, even if this were the case, these elements not being the C-S-H (main phase of cement hardening), their action on the mechanical properties remains in conformity with the results obtained.

Regarding the analysis of C-S-H peaks, this work as well as many others [9, 60] agrees that C-S-H is amorphous, and its study using X-ray diffractograms is difficult. The filler effect (strongly influenced by the particle size), remains the central element that determines the effect of waste gneiss powder on the properties of mortars.

6. Conclusion

In the end, this work aimed to characterize a gneiss sample, show the engineering properties of gneiss powder in cement matrices, and rule on the pozzolanic effect of this drilling waste produced in gneiss quarries as a cement additive. After having proceeded to geological mapping of the site, the macroscopic description identified this massif as being a crystalline metamorphic rock. The structural study revealed veins, folds, foliations, joints, and breaks. The major discontinuities after measurement were oriented N180°. Thin section analysis performed on the rock samples identified quartz (Qt), plagioclase (Pl), mica (Mi), muscovite (Mu), orthopyroxene (Px), and biotite (Bt) which are characteristic of Gneiss. The chemical and mineralogical analysis carried out confirmed the presence of these minerals. Once the massif was identified, the waste gneiss powders were collected in 10 boreholes made for blasting. The classification showed that

they consisted largely of fines that could be used in mortars, like Basalt powder and Granite powder in other works.

The cement employed, CPJ CEM II/A-P 42.5R, had a specific gravity of 2.98 and a Blaine-specific surface area of 3353 cm^2/g. Based on the results of the chemical investigation, Bogue calculations revealed that the cement was predominantly alite (62.02%). The hydraulic modulus of 2.3 suggested that early-age strengths were low. The hydraulic index of 0.37 indicated that this cement was likely to have good water resistance.

The addition of gneiss powder to the cement paste increased the setting time from 225 minutes for 10% cement replacement to 285 minutes for 50% substitution, a 15-minute increase on average. This increase was mostly related to cement particle dispersion by gneiss particles. Water absorption data revealed that the rate of absorption decreased proportionally to the percentage of addition. This increased from 4.69% (OPC) to 1.97% (50% addition) after 2 days, 5.16% (OPC) to 2.07% (50% addition) after 7 days, and 6.05% (OPC) to 2.36% (50% addition) after 28 days. The mechanical results of mortars decreased as the substitute proportion increased. Indeed, the compressive strengths fell from -3.33% to -20.00% after 28 days for 10% and 50% substitution, respectively. At 10% substitution, flexural strength improvements of 2.22% and 1.89% were seen during 2 and 7 days of cure, highlighting the filler impact. The filler effect explained that despite this loss of strength, the proportion of loss remained very far from the percentage of substitution. The inclusion of gneiss powder enhanced C3A and C4AF content due to the contribution of aluminous minerals detected in the gneiss, according to mineralogical study. This inclusion had little or no effect on the generation of CSH peaks, according to the analysis. This finding corroborated the hypothesis of gneiss powder's very probable inertia in cementitious matrices and limited its positive effect to the filler effect of fine particles.

Consequently, while adding gneiss dust to cement is a method of recycling this waste material without significantly reducing mortar strength, this application must be dimensioned to guarantee that items such as blocks or other cement products meet the technical criteria of their intended use. As a result, it appears suitable to do additional research on the particle size range that provides the best filler effect and durability of cement matrices with the inclusion of gneiss powder. Work on ternary cement with the inclusion of gneiss powder and a material expected to create a stronger pozzolanic effect might also be done to improve the quality of this green mortar.

Acknowledgments

The Authors are grateful to Professor Nathalie Fagel (AGES Lab), University of Liege, Belgium, for her assistance in conducting some analyses in her Institution**.** We dedicate this effort to the memory of our colleague Bodang Mikael Moudoh, with whom we had fruitful collaboration throughout our research journey.

Author Contributions Tchedele Langollo Yannick: Validation, Methodology, Writing - review & editing, Visualization, original draft, Matateyou Josephine Fleure: Conceptualization, Methodology, Investigation, Writing - original draft. Robert Mba Eboe: Validation, Writing - review & editing, Visualization... Taypondou Darman Japhet: Methodology, Writing review & editing, original draft Atsafoue Donfack Sandrine: Methodology, Investigation, review & editing, Abende Sayom Yvan Reynolds: Supervision, Methodology, Resources, Keyangue Tchouata Jules Hermann: Supervision, Methodology, Resources.

Funding The authors received no financial support for the research, authorship, and/or publication of this article.

Data Availability All data generated or analyzed during this study are included in this article.

Compliance with Ethical Standards This manuscript has not been published elsewhere in any form or language and has not been submitted to more than one journal for simultaneous consideration.

Declaration on Conflict of Interest The authors declare that they have no conflict of interest.

Code Availability Not applicable.

Consent to Participate Not applicable.

Consent for Publication Not applicable.

References

[1] Piedou, J. (1996). *Dépoussiérage en carrière*. Mines et Carrières. vol. 78.

[2] Gupta, L. K., & Vyas, A. K. (2018). Impact on mechanical properties of cement sand mortar containing waste granite powder. *Construction and Building Materials*, *191*, 155-164. https://doi.org/10.1016/j.conbuildmat.2018.09.203

[3] Cui, L., Chen, P., Wang, L., Xu, Y., & Wang, H. (2022). Reutilizing Waste Iron Tailing Powders

as Filler in Mortar to Realize Cement Reduction and Strength Enhancement. *Materials*, *15*(2), 541. https://doi.org/10.3390/ma15020541

[4] Tchedele, L. Y., Mambou, N. L. L., Kamga, S. L. V. E., Tchamba, A. B., Ngounouno, I. & Bier. A. T. (2020). *Mechanical and Microstructutral properties of Cameroonian CPJ NC CEM II/B-P 42.5R cement substitution by glass powder in the cement paste and mortar*. SN applied Science. 2:1368. P.12.https://doi.org/10.1007/s42452-020-3152-y.

[5] Sales, R. B. C., Sales, F. A., Figueiredo, E. P., dos Santos, W. J., Mohallem, N. D. S., & Aguilar, M. T. P. (2017). Durability of Mortar Made with Fine Glass Powdered Particles. *Advances in Materials Science and Engineering*, *2017*, 1-9. https://doi.org/10.1155/2017/3143642

[6] Dobiszewska, M., Pichór, W., & Szołdra, P. (2019). Effect of basalt powder addition on properties of mortar. *MATEC Web of Conferences*, *262*, 06002. https://doi.org/10.1051/matecconf/201926206002

[7] Unčík, S., & Kmecová, V. (2013). The Effect of Basalt Powder on the Properties of Cement Composites. *Procedia Engineering*, *65*, 51-56. https://doi.org/10.1016/j.proeng.2013.09.010

[8] Jain, K. L., Sancheti, G., & Gupta, L. K. (2020). Durability performance of waste granite and glass powder added concrete. *Construction and Building Materials*, *252*, 119075. https://doi.org/10.1016/j.conbuildmat.2020.119075

[9] Ramadji, C., Messan, A., & Prud'Homme, E. (2020). Influence of Granite Powder on Physico-Mechanical and Durability Properties of Mortar. *Materials*, *13*(23), 5406. https://doi.org/10.3390/ma13235406

[10] Lezzerini, M., Luti, L., Aquino, A., Gallello, G., & Pagnotta, S. (2022). Effect of Marble Waste Powder as a Binder Replacement on the Mechanical Resistance of Cement Mortars. *Applied Sciences*, *12*(9), 4481. https://doi.org/10.3390/app12094481

[11] Amin, S. K., Allam, M. E., Garas, G. L., & Ezz, H. (2020). A study of the chemical effect of marble and granite slurry on green mortar compressive strength. *Bulletin of the National Research Centre*, *44*(1), 19. https://doi.org/10.1186/s42269-020-0274-8

[12] Nasr, M. S., Shubbar, A. A., Abed, Z. A.-A. R., & Ibrahim, M. S. (2020). Properties of eco-friendly cement mortar contained recycled materials from different sources. *Journal of Building Engineering*, *31*, 101444. https://doi.org/10.1016/j.jobe.2020.101444

[13] Omar, O. M., Abd Elhameed, G. D., Sherif, M. A., & Mohamadien, H. A. (2012). Influence of limestone waste as partial replacement material for sand and marble powder in concrete properties. *HBRC Journal*, *8*(3), 193-203. https://doi.org/10.1016/j.hbrcj.2012.10.005

[14] Hewlett, P., & Liska, M. (Eds.). (2019). *Lea's chemistry of cement and concrete*. Butterworth-Heinemann.

[15] Martinez, C. M., del Bosque, I. S., Medina, G., Frías, M., & de Rojas, M. S. (2021). Fillers and additions from industrial waste for recycled aggregate concrete. *The Structural Integrity of Recycled Aggregate Concrete Produced with Fillers and Pozzolans*, 105-143.

[16] Holland, B., Alapati, P., Kurtis, K. E., & Kahn, L. (2023). Effect of different concrete materials on the corrosion of the embedded reinforcing steel. *Corrosion of Steel in Concrete Structures*, 199-218

[17] Habert, G. (2014). Assessing the environmental impact of conventional and 'green'cement production. In *Eco-efficient construction and building materials* (pp. 199-238). Woodhead Publishing.

[18] Gayarre, F. L., Boadella, I. L., Gonzalez, J. S., Lopez-Colina, C., Lopez, M. S., & Stochino, F. (2021). Waste for aggregates in ultrahigh performance concrete (UHPC). In *Waste and Byproducts in Cement-Based Materials* (pp. 29-51). Woodhead Publishing.

[19] Maurizot p., Abessolo, a., Feybesse, a., Johan, v. et Lecomte, p. (1986). *Étude et prospection minière du Sud-Ouest Cameroun. Synthèse des travaux de 1978-1985.* Bureau de Recherches Geologiques et Minieres, BRGM 85 CMR 066, Orleans, France, 274 p.

[20] Nzenti J.P., T. Njanko, E.L.T. Njiosseu et Thoua, F.M. (1998). *Les domaines granulitiques de la chaine panafricaine nord-equatoriale au Cameroun.* Dans : Géologie et environnement au Cameroun, J.P. VICAT et P. BILONG (Editeurs), Collection GEOCAM 1, Presses Universitaires de Yaounde I, Yaounde, Cameroun, pp. 255-264.

[21] Owona S., Mvondo, O.J, Essono, J., Tjomb B., et. Enama M.M. (2003). *Geomorphologie et cartographie de deux facies paraderives et un orthoderive de la region de Yaounde*. J. STD, 10, Pp.81-91.

[22] Mvondo H., Owona, S., Mvondo O.J. et Essono, J. (2007). *Tectonic evolution of the Yaounde segment of the Neoproterozoic Central Orogenic Belt in southern Cameroun*. Can. J. Earth Sci., 44, Pp. 433-444.

[23] NF EN 197-1 (2012). Ciment - Partie 1 : composition, spécifications et critères de conformité des ciments courants. *AFNOR.*

[24] EN 196-1 (2005), Methods of testing cement. Determination of strength, *CEN.*

[25] NF EN 933-1 (2012) Essais pour déterminer les caractéristiques géométriques des granulats - Partie 1 : détermination de la granularité - Analyse granulométrique par tamisage. *AFNOR.*

[26] NF EN 933-2 (2020). Essais pour déterminer les caractéristiques géométriques des granulats - Partie 2 : détermination de la granularité - Tamis de contrôle, dime nsions nominales des ouvertures. *AFNOR.*

[27] NF EN 196-6 (2018). Méthodes d'essai des ciments - Détermination de la masse volumique apparente. *AFNOR.*

[28] NF EN 196-6 (2018). Méthodes d'essai des ciments - Détermination de la masse volumique absolue. *AFNOR.*

[29] NF EN 196-6 (2018). Méthodes d'essai des ciments - Détermination de la finesse. *AFNOR.*

[30] Newman, J. and Choo, S. B. (2003). Advanced concrete technology, constituent materials. *Elsevier*, Burlington.

[31] Bogue, R. H. (1955). The chemistry of Portland cement, *LWW*, 79(4), 322.

[32] NF EN 196-3 (2017). Méthodes d'essai des ciments - Partie 3 : détermination du temps de prise et de la stabilité. *AFNOR*.

[33] ASTM C642 – 13 (2013). Standard Test Method for Density, Absorption, and Voids in Hardened Concrete, *ASTM International*, West 433Conshohocken, USA.

[34] Mambou, N.L.L., Ndop, J., Ndjaka, B. (2017). Investigations of thermal damage on the physical and mechanical properties of gneiss rock specimen. *J Powder Metall Min*, *6*(3), 1-6.

[35] Ndjigui, P. D., Badinane, M. F. B., Nyeck, B., Nandjip, H. P. K., & Bilong, P. (2013). Mineralogical and geochemical features of the coarse saprolite developed on orthogneiss in the SW of Yaoundé, South Cameroon. *Journal of African Earth Sciences*, *79*, 125-142.

[36] Mboudou, M. G. M., Sebastien, O., Moussa, N. N., Cyrille, S., Christian, B. A., & Guilliano, F. (2022). Petrology and feldspar chemistry of the Penja–Manjo pegmatites in the Pan-African orogenic belt of Cameroon: economic implication. *Arabian Journal of Geosciences*, *15*(7), 570.

[37] Kamgang Tchuifong, B. A., Jules, T. K., Martial, F. E., Ludovic, A. M., Julios, E. A., Robinson, S. B., Safianou, O., Maurice, K. (2023). Geological mapping and structural interpretation of the Dschang-Santchou-escarpment (West, Cameroon), using Landsat 8 OLI/TIRS sensors/SRTM and field observations. *Geological Journal*, *58*(3), 1111-1130.

[38] Nyeck, B., Ngimbous, R. V., & Ndjigui, P. D. (2019). Petrology of saprolite developed on gneisses in the Matomb region, south Cameroon. *Journal of African Earth Sciences*, *150*, 107-122.

[39] Fuanya, C., Bolarinwa, A. T., Kankeu, B., Yongue, R. F., Tangko, E. T., & Nkepguep, F. Y. (2019). Geochemical characteristics and petrogenesis of basic rocks in the Ako'ozam–Njabilobe area, Southwestern Cameroon: implications for Au genesis. *SN Applied Sciences*, *1*, 1-12.

[40] Nzenti, J. P., Barbey, P., Macaudiere, J., & Soba, D. (1988). *Origin and evolution of the late precambrian high grade Yaounde Gneisses (Cameroon).* Precambrian Research, *38*(2), 91-109. https://doi.org/10.1016/0301-9268(88)90086-1

[41] NF EN 12620 (2008). Granulats pour béton, *AFNOR*.

[42] Duna, L. L., Nguimeya, N. G. A., Tchamba, A. B., Billong, N., Kamseu, E., Qoku, E., Alomayri, T. S., Bier, T. A. (2022). Engineering and mineralogical properties of Portland cement used for building and road construction in Cameroon. *International Journal of Pavement Research and Technology*, 15(4), 821-834.

[43] Mambou, N. L. L., Tchapga, G. G. M., Ndop, J., Fofe, M. C. and Ndjaka, J. M. B. (2017). A Comparative Study of Concrete Strength Using Metamorphic, Igneous, and Sedimentary

Rocks (Crushed Gneiss, Crushed Basalt, Alluvial Sand) as Fine Aggregate, *Journal of Architectural Engineering Technology*, *6*(1), 1-6.

[44] Mambou. N. L. L., Fotseu, M. C. D., Kamseu, E. (2019). Valorization of wood ashes as partial replacement of Portland cement: mechanical performance and durability. *European Journal of Scientific Research*, 151(4), 468-478.

[45] Elaqra, H. and Rustom, R. (2018). Effect of using glass powder as cement replacement on rheological and mechanical properties of cement paste, *Construction and Building Materials*, vol. 179, 326-335.

[46] Dunuweera, S. P., and Rajapakse, R. M. G. (2018). Cement types, composition, uses and advantages of nanocement, environmental impact on cement production, and possible solutions. *Advances in Materials Science and Engineering*, https://doi.org/10.1155/2018/4158682

[47] Samen, K. L. V. E., Yanou, R. N., Fonzeu C. K. M., Kamgue L. A. R., Tchamba, A. B., Tchapga G. G. M., Yang, L., Mempouo, B. (2022). Engineering properties of soda-lime glass powder on Portland cement CEM IV-B-L mortar, *Journal of Building Pathology and Rehabilitation*, 7(27), 15. https://doi.org/10.1007/s41024-022-00164-3

[48] Bombled, J.P. (1964). Rhéologie du béton frais, Publication Technique N°161, *C.E.R.I.L.H.*, Paris.

[49] Katz, A., Kulisch, D., (2017). *Performance of mortars containing recycled fine aggregate from construction and demolition* waste. Mater. Struct. 50 (4), 199.

[50] Munoz-Ruiperez, C., Rodriguez, A., Gutierrez-Gonzalez, S., Calderon, V., (2016). *Lightweight masonry mortars made with expanded clay and recycled aggregates*. Constr. Build. Mater. 118, 139e145.

[51] Kim, H.K., Ha, K.A., Lee, H.K., (2016). *Internal-curing efficiency of cold-bonded coal bottom ash aggregate for high-strength mortar*. Constr. Build. Mater. 126, 1e8.

[52] Xie Z, Xi Y (2002) *Use of recycled glass as a raw material in the manufacture of Portland cement.* Mater Struct 35:510–515.

[53] Hwang CL, Shen DH (1991) *The effects of blast-furnace slag and fly ash on the hydration of Portland cement.* Cem Concr Res 21(4):410–425.

[54] Li, L.G.; Wang, Y.M.; Tan, Y.P.; Kwan, A.K.H.; Li, L.J. (2018). *Adding granite dust as paste replacement to improve durability and dimensional stability of mortar*. Powder Technol., 333, 269–276.

[55] Xiao, Z.Y.; Xu,W. (2019) *Assessment of strength development in cemented coastal silt admixed granite powder*. Constr. Build. Mater., 206, 470–482.

[56] Reiterman P., Jaskulski R., Kubissa W., Holčapek O., Keppert M. (2020). *Assessment of Rational Design of Self-Compacting Concrete Incorporating Fly Ash and Limestone Powder in Terms of Long-Term Durability*. Materials.;13:2863. doi: 10.3390/ma13122863.

[57] Arulraj G.P., Adin A., Kannan T.S. (2013) *Granite Powder Concrete*. IRACST–Eng. Sci. Technol. Int. J. ESTIJ.;3:193–198.

[58] V.G. Haach, G. Vasconcelos, P.B. Loureno, (2011) *Influence of aggregates grading and water/cement ratio in workability and hardened properties of mortars*, Constr. Build. Mater. 25 2980–2987, https://doi.org/10.1016/j.conbuildmat. 2010.11.011.

[59] Lalan, P. (2016) *Influence d'une Température de 70 _C sur la Géochimie, la Microstructure et la Diffusion Aux Interfaces Béton/Argile: Expérimentations en Laboratoire, In Situ et Modélisation*. Available online: https://www.irsn.fr/FR/Larecherche/Formation_recherche/Theses/Theses-soutenues/PRP-DGE/Pages/2016-Lalan-influence-temperature-70-geochimie-microstructure-di_usion-interfaces-beton-argile.aspx#.X5jeFO0RVPY (accessed on 26 August 2020).

[60] Choudhary, H.K., Anupama, A.V., Kumar, R., Panzi, M.E., Matteppanavar, S., Sherikar, B.N., Sahoo, B. (2015). Observation of phase transformations in cement during hydration, Constr. Build. Mater. 101, 122–129, https://doi.org/10.1016/ j.conbuildmat.2015.10.027.